Electronic Supplementary Material (ESI) for Dalton Transactions.
This journal is © The Royal Society of Chemistry 2020

Electronic Supplementary Information on

$(HPy)_2(Py)CuBi_3I_{12}$, a Low Bandgap Metal Halide Photoconductor

Jakob Möbs,[†] *Marina Gerhard,*[‡] *Johanna Heine*,*[†]

[†] Department of Chemistry and Material Sciences Center, Philipps-Universität Marburg,
Hans-Meerwein-Straße, 35043 Marburg, Germany.

[‡] Department of Physics and Material Sciences Center, Philipps-Universität Marburg,
Renthof 7, 35032 Marburg, Germany.

Table of Contents

Synthesis

BiI_3 was synthesized from the elements according to literature procedures.[1] Bi_2O_3, CuI, HI (57 % solution in water, stabilizer: 0.75 % H_3PO_2) and acetic acid (p. a.) were used as supplied from commercial sources. Ethanol (EtOH), diethyl ether (Et_2O), 1,2-dimethoxyethane (dme), *n*-pentane and pyridine (Py) were generally flash-distilled prior to use. HPyI was prepared by mixing aqueous HI and pyridine in equimolar ratios in Et_2O. The precipitate was filtered of, washed with Et_2O and dried under vacuum. CHN analysis was carried out on an Elementar CHN-analyzer.

$(HPy)_2(Py)CuBi_3I_{12}$ (1). A total of 118 mg of BiI_3 (0.2 mmol), 12.5 mg of CuI (0.066 mmol) and 27.5 mg of HPyI (0.133 mmol) were suspended in 5 mL of ethanol. 5.3 µL of pyridine (0.066 mmol) were added under stirring and the mixture was heated to 80 °C for 6 h under reflux cooling. Afterwards the suspension was stirred at room temperature for additional 12 h. The black precipitate was collected, washed once with 5 mL of cold ethanol and thrice with 5 mL of *n*-pentane. After drying under vacuum 147 mg (91 %) of **1** were obtained as reddish black powder. CHN (calculated for $C_{15}H_{17.2}Bi_3Cu_{0.8}I_{12}N_3$, see below): C 7.63 (7.38), H 0.64 (0.71), N 1.70 (1.72). It should be noted that we found this synthesis to be easily upscalable to at least the ten-fold amount.

Single crystals were obtained by layering a solution of the starting materials in dme with *n*-pentane.

During our experiments, we found different values for the degree of occupation of the copper position. The two single crystal measurements suggest occupations of 60 % and 50 % (see also *Crystallographic Details*). Since both crystals were produced in the same experiment this points to a range of possible degrees of occupation. Thermal analysis (see below) of the crystals grown from dme/*n*-pentane supports these values as it gives an average occupation of 55 % which corresponds to the sum formula $C_{15}H_{16.9}Bi_3Cu_{1.1}I_{12}N_3$. In contrast to that, thermal analysis of the bulk product suggests an occupation of only 40 % ($C_{15}H_{17.2}Bi_3Cu_{0.8}I_{12}N_3$). We assign the differences in the copper content to the significantly lower solubility of CuI in ethanol compared to dme. We also tried to increase the copper content of the bulk product by increasing the initial amount of CuI in the reaction, but then always found the product to be contaminated with CuI.

$(HPy)_3Bi_2I_9$ (2). A total of 92 mg of Bi_2O_3 (0.2 mmol) were suspended in 10 mL of aqueous HI (c = 2 mol/L). Under stirring 48.4 µL of pyridine (0.6 mmol) were added and the mixture was heated to 90 °C for 30 min under reflux cooling. The resulting clear red solution was left for crystallization at room temperature. After two days large red crystals of **2** had formed. The solvent was decanted, the crystals rinsed twice with 5 mL of acetic acid and dried under vacuum yielding 147 mg (41 %) of crystalline product. CHN (calculated for $C_{15}H_{18}Bi_2I_9N_3$): C 10.29 (10.01), H 1.02 (1.01), N 2.28 (2.33).

In addition to compound **1** and **2**, we also obtained a number of different pyridinium iodido bismuthates during our experiments as side products while exploring different reaction conditions. All of them feature anion motifs that have been observed frequently already in the chemistry of iodido bismuthates, so we include their single crystal structures here for the sake of completeness and to help other researchers who want to prepare multinary iodido bismuthates with pyridinium as a counterion. We also tried to obtain copper iodio antimonates in the same way as compound **1** using SbI_3 instead of BiI_3, but we could only obtain compounds with binary iodido antimonate anions. Similar to the iodido bismuthates, the anion motifs in these compound are also well-known and we include the novel single crystal structures we obtained here for the sake of completeness. As all of these compounds are of lesser interest in the context of our search for new compounds with ternary anions, we did not optimize their synthesis. They generally crystallized within a few days to a few weeks from solutions of pentel iodides, coinage metal iodides and HPyI in acetonitrile, acetone, 1,2-dimethoxyethane or aqueous HI, which were dissolved by heating under reflux cooling for about an hour.

Crystallographic Details

Single crystal X-ray determination was performed on a Bruker Quest D8 diffractometer with microfocus MoKα radiation (λ = 0.71073) and a Photon 100 (CMOS) detector or a STOE IPDS-2/2T diffractometer equipped with an imaging plate detector system using MoKα radiation with graphite monochromatization.

Table S1: Crystallographic data for $C_{15}H_{16.8}Bi_3Cu_{1.2}I_{12}N_3$ (**1**), measured on a Bruker Quest D8 at 100 K, CCDC 2025570.

Empirical formula	$C_{15}H_{16.8}Bi_3Cu_{1.2}I_{12}N_3$
Formula weight	2465.10
Crystal system	triclinic
Space group	*P*-1
a/Å	9.9152(5)
b/Å	10.0648(5)
c/Å	11.4957(6)
α/°	64.8710(10)
β/°	78.306(2)
γ/°	85.680(2)
Volume/Å^3	1017.00(9)
Z	1
ρ_{calc}/g/cm^3	4.025
μ/mm^{-1}	22.676
F(000)	1048.0
Crystal size/mm^3	0.066 × 0.044 × 0.02
Absorption correction (T_{min}/T_{max})	multi-scan (0.0557/0.0915)
2Θ range for data collection/°	4.47 to 50.628
Index ranges	$-11 \leq h \leq 11$, $-12 \leq k \leq 12$, $-13 \leq l \leq 13$
Reflections collected	39268
Independent reflections	3686 [R_{int} = 0.0784, R_{sigma} = 0.0345]
Data/restraints/parameters	3686/0/145
Goodness-of-fit on F^2	1.074
Final R indexes [I>=2σ (I)]	R_1 = 0.0364, wR_2 = 0.0534
Final R indexes [all data]	R_1 = 0.0539, wR_2 = 0.0568
Largest diff. peak/hole / e Å^{-3}	2.11/-1.41

Details of crystal structure refinement: All non-hydrogen atoms were refined anisotropically with the exception of the carbon and nitrogen atoms in one of the pyridinium moieties that was disordered across the center of inversion. Hydrogen atoms were assigned to idealized geometric positions and included in structure factors calculations. The occupancy of the Cu position (Cu1) was first refined freely, then fixed to the closest single digit occupancy value (0.6). The corresponding hydrogen atom (H1) was set to an occupancy of 0.4. An AFIX 66 command was used on the disordered pyridinium cation to ensure a stable refinement.

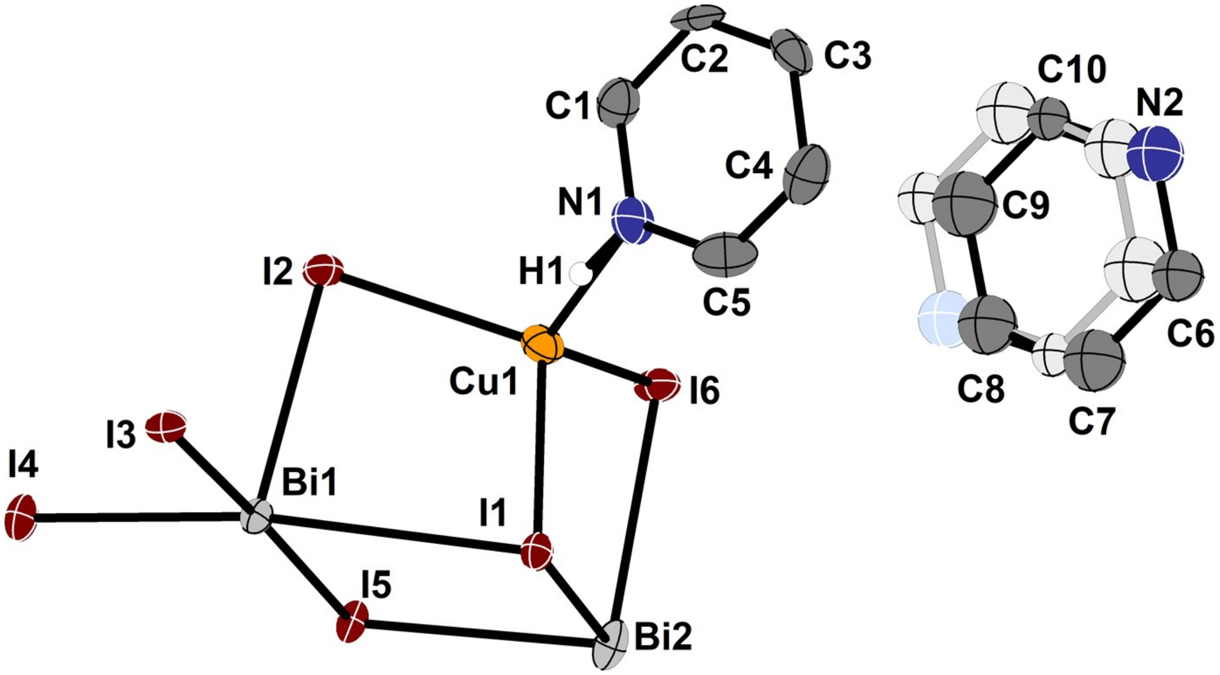

Figure S1: Asymmetric unit of **1**, ellipsoids at 50 % probability. Only hydrogen atom H1 is shown for clarity. The second position of the disordered pyridinium moiety is shown in lighter colors.

Table S2: Crystallographic data for $C_{15}H_{17}Bi_3CuI_{12}N_3$ (**1**), measured on a Bruker Quest D8 at 293 K, CCDC 2025571.

Empirical formula	$C_{15}H_{17}Bi_3CuI_{12}N_3$
Formula weight	2452.59
Crystal system	triclinic
Space group	*P*-1
a/Å	9.9874(6)
b/Å	10.1149(6)
c/Å	11.6385(7)
α/°	65.080(2)
β/°	78.747(2)
γ/°	86.282(2)
Volume/Å^3	1045.58(11)
Z	1
ρ_{calc}/g/cm^3	3.895
μ/mm^{-1}	21.957
F(000)	1042.0
Crystal size/mm^3	0.31 × 0.274 × 0.054
Absorption correction (T_{min}/T_{max})	multi-scan (0.0029/0.0185)
2Θ range for data collection/°	4.442 to 50.574
Index ranges	$-11 \leq h \leq 11$, $-11 \leq k \leq 12$, $-13 \leq l \leq 13$
Reflections collected	21510
Independent reflections	3774 [$R_{int} = 0.0594$, $R_{sigma} = 0.0368$]
Data/restraints/parameters	3774/108/163
Goodness-of-fit on F^2	1.168
Final R indexes [I>=2σ (I)]	$R_1 = 0.0484$, $wR_2 = 0.1134$
Final R indexes [all data]	$R_1 = 0.0642$, $wR_2 = 0.1195$
Largest diff. peak/hole / e Å^{-3}	1.00/-1.60

Details of crystal structure refinement: All non-hydrogen atoms were refined anisotropically. Hydrogen atoms were assigned to idealized geometric positions and included in structure factors calculations. The occupancy of the Cu position (Cu1) was first refined freely, then fixed to the closest single digit occupancy value (0.5). The corresponding hydrogen atom (H1) was set to an occupancy of 0.5. An AFIX 66 command was used on both pyridine/pyridinium moieties to ensure a stable refinement. SIMU, RIGU and ISOR commands had to be used on the atoms of the pyridinium moiety which is disordered about the center of inversion. The shape of the ellipsoids of this moiety suggest that additional disorder is present, which we have not modelled for the sake of refinement stability.

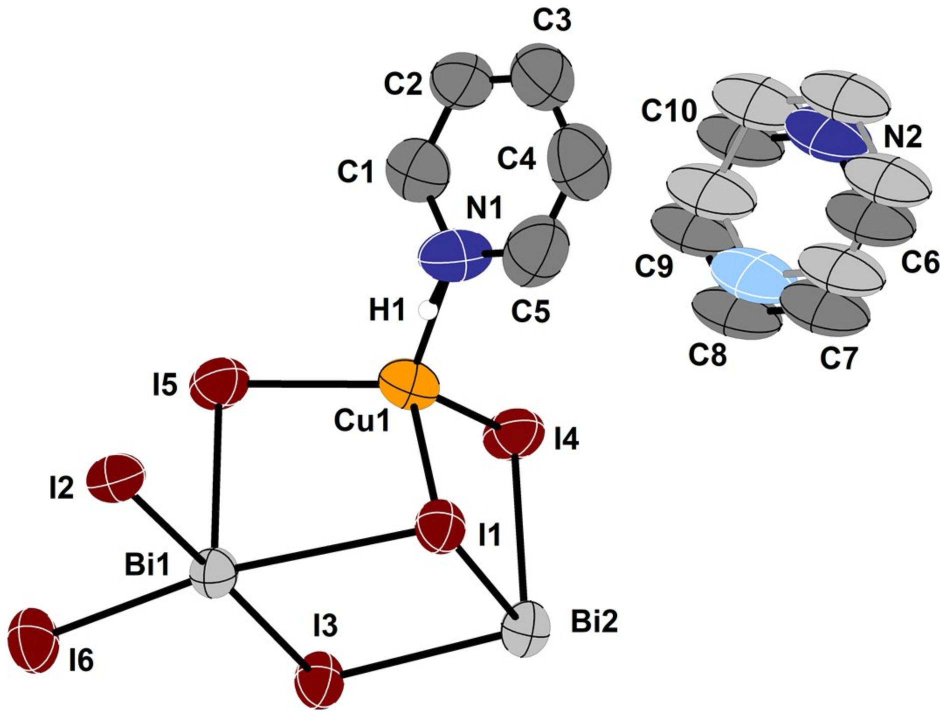

Figure S2: Asymmetric unit of **1** at 293 K, ellipsoids at 50 % probability. Only hydrogen atom H1 is shown for clarity. The second position of the disordered pyridinium moiety is shown in lighter colors.

Table S3: Comparison of bond lengths in **1** (at 100 K) with $(Cu(CH_3CN)_4)_2Cu_2Bi_2I_{10}$ and $(n\text{-}Bu_4N)_2(CH_3CN)_2Cu_2Bi_2I_{10}$. [2]

	1	$\mathbf{(Cu(CH_3CN)_4)_2Cu_2Bi_2I_{10}}$	$\mathbf{(\mathit{n}\text{-}Bu_4N)_2(CH_3CN)_2Cu_2Bi_2I_{10}}$
Bi-I / Å	2.865-3.353	2.923-3.334	2.903-3.322
Cu-I /Å	2.637-2.683	2.616-2.685	2.650-2.696
Cu-N /Å	2.001	1.969-2.034	2.000

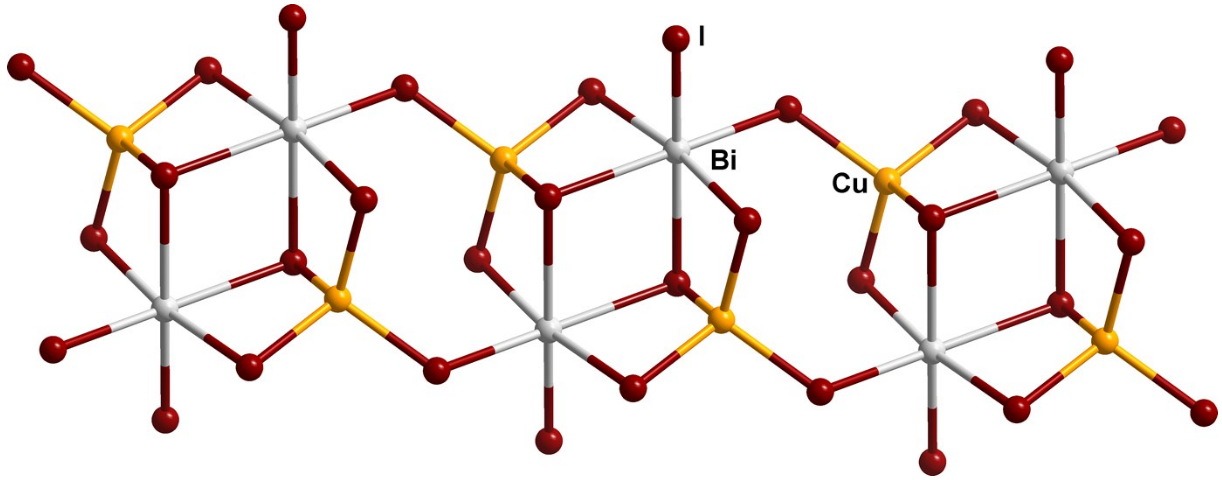

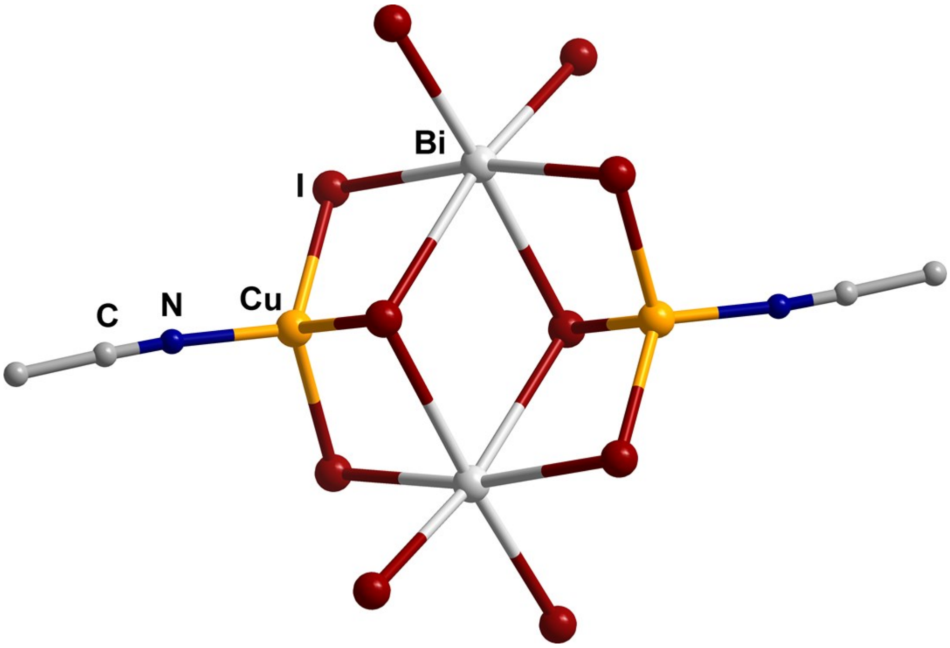

Figure S3: Excerpts of the crystal structures of literature compounds $(Cu(CH_3CN)_4)_2Cu_2Bi_2I_{10}$ (top) and $(n\text{-}Bu_4N)_2(CH_3CN)_2Cu_2Bi_2I_{10}$ (bottom) showing the anion motifs.[2]

Table S4: Crystallographic data for $C_{15}H_{18}Bi_2I_9N_3$ (**2**), measured on a Bruker Quest D8 at 100 K, CCDC 2025572.

Empirical formula	$C_{15}H_{18}Bi_2I_9N_3$
Formula weight	1800.38
Crystal system	orthorhombic
Space group	*Pnma*
a/Å	14.6088(6)
b/Å	23.6348(9)
c/Å	9.9053(4)
α/°	90
β/°	90
γ/°	90
Volume/Å^3	3420.1(2)
Z	4
ρ_{calc}/g/cm^3	3.497
μ/mm^{-1}	18.41
F(000)	3088.0
Crystal size/mm^3	0.109 × 0.08 × 0.026
Absorption correction (T_{min}/T_{max})	multi-scan (0.5341/0.7452)
2Θ range for data collection/°	4.458 to 50.612
Index ranges	$-17 \leq h \leq 17$, $-28 \leq k \leq 28$, $-13 \leq l \leq 11$
Reflections collected	53765
Independent reflections	3188 [$R_{int} = 0.1239$, $R_{sigma} = 0.0390$]
Data/restraints/parameters	3188/13/140
Goodness-of-fit on F^2	1.073
Final R indexes [I>=2σ (I)]	$R_1 = 0.0320$, $wR_2 = 0.0430$
Final R indexes [all data]	$R_1 = 0.0535$, $wR_2 = 0.0468$
Largest diff. peak/hole / e Å^{-3}	0.93/-1.01

Details of crystal structure refinement: All non-hydrogen atoms were refined anisotropically. Hydrogen atoms were assigned to idealized geometric positions and included in structure factors calculations. Since one of the pyridinium cations is disordered about the center of an inversion, C6 and N2 share the same position and both have an occupancy of 0.5. The position was refined using EYXZ and EADP commands and an additional ISOR command had to be used to give meaningful anisotropic displacement parameters.

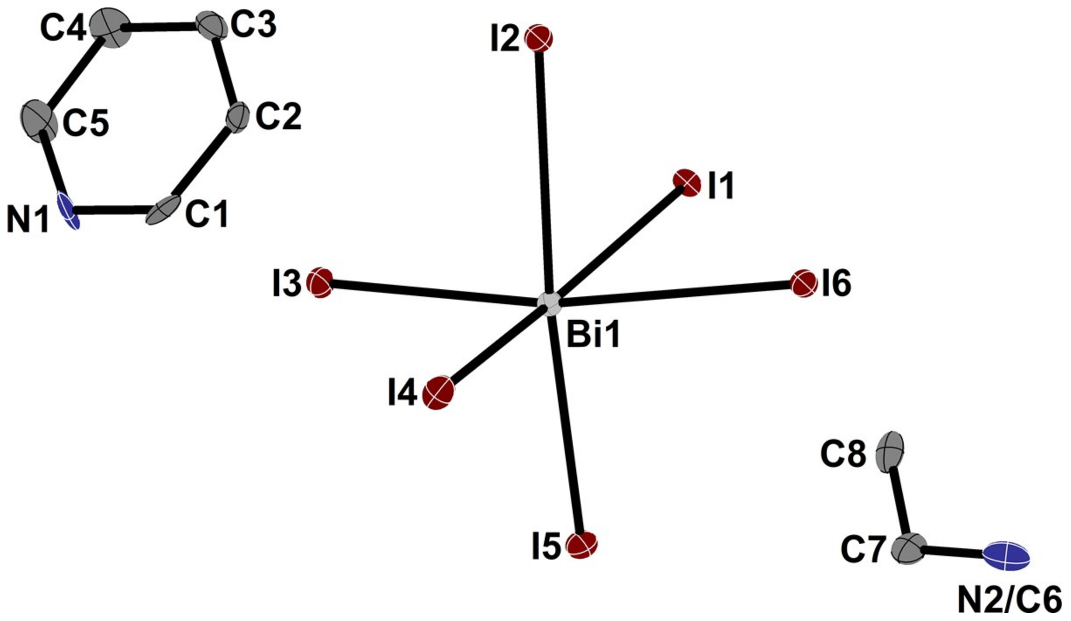

Figure S4: Asymmetric unit of **2**, ellipsoids at 50 % probability. Hydrogen atoms are omitted for clarity.

Table S5: Crystallographic data for $C_{23}H_{38}Bi_2I_9N_3O_4$ (**3-Bi**), measured on a Stoe IPDS-2/2T at 100 K, CCDC 2025573.

Empirical formula	$C_{23}H_{38}Bi_2I_9N_3O_4$
Formula weight	1980.62
Crystal system	orthorhombic
Space group	$C222_1$
a/Å	8.5623(6)
b/Å	18.8440(10)
c/Å	28.796(2)
α/°	90
β/°	90
γ/°	90
Volume/Å^3	4646.2(5)
Z	4
ρ_{calc}g/cm^3	2.831
μ/mm^{-1}	13.572
F(000)	3488.0
Crystal size/mm^3	0.1905 × 0.099 × 0.08
Absorption correction (T_{min}/T_{max})	numerical (0.2975/0.4012)
2Θ range for data collection/°	2.8 to 53.7
Index ranges	$-10 \leq h \leq 10$, $-21 \leq k \leq 23$, $-36 \leq l \leq 36$
Reflections collected	19966
Independent reflections	4939 [$R_{int} = 0.0933$, $R_{sigma} = 0.0766$]
Data/restraints/parameters	4939/89/215
Goodness-of-fit on F^2	0.954
Final R indexes [I>=2σ (I)]	$R_1 = 0.0346$, $wR_2 = 0.0806$
Final R indexes [all data]	$R_1 = 0.0478$, $wR_2 = 0.0827$
Largest diff. peak/hole / e Å^{-3}	2.11/-1.93
Flack parameter	-0.026(5)

Details of crystal structure refinement: All non-hydrogen atoms were refined anisotropically. Hydrogen atoms were assigned to idealized geometric positions and included in structure factors calculations. SIMU, RIGU SADI and FLAT commands as implemented in the FragmentDB / DSR[3] had to be used on the atoms of the pyridinium cation which is disordered about the center of inversion.

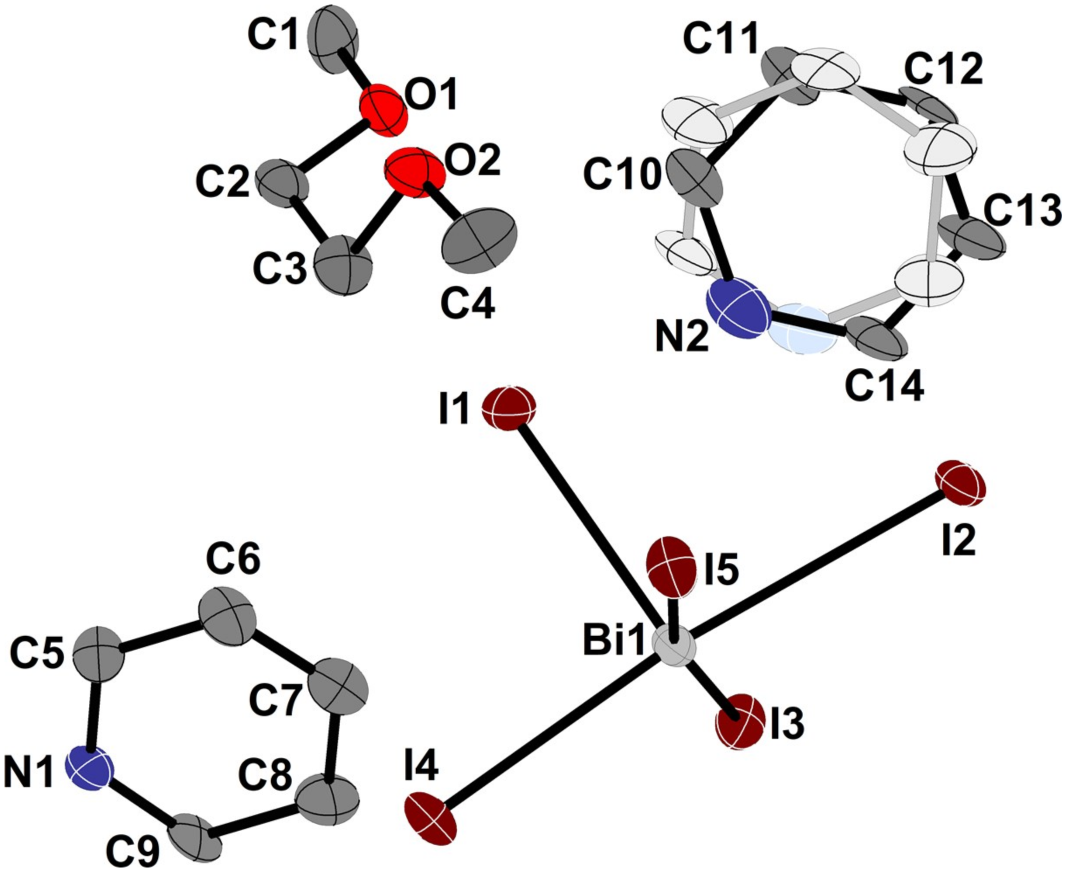

Figure S5: Asymmetric unit of **3-Bi**, ellipsoids at 50 % probability. Hydrogen atoms are omitted for clarity. The second position of the disordered pyridinium moiety is shown in lighter colors.

Table S6: Crystallographic data for $C_{23}H_{38}I_9N_3O_4Sb_2$ (**3-Sb**), measured on a Stoe IPDS-2/2T at 100 K, CCDC 2025574.

Empirical formula	$C_{23}H_{38}I_9N_3O_4Sb_2$
Formula weight	1806.16
Crystal system	orthorhombic
Space group	$C222_1$
a/Å	8.5313(5)
b/Å	18.8548(10)
c/Å	28.583(2)
α/°	90
β/°	90
γ/°	90
Volume/Å^3	4597.8(5)
Z	4
ρ_{calc}/g/cm^3	2.609
μ/mm^{-1}	7.246
F(000)	3232.0
Crystal size/mm^3	0.29738 × 0.24907 × 0.16201
Absorption correction (T_{min}/T_{max})	numerical (0.1840/0.3653)
2Θ range for data collection/°	2.85 to 53.954
Index ranges	$-10 \le h \le 10$, $-23 \le k \le 18$, $-36 \le l \le 36$
Reflections collected	13992
Independent reflections	4906 [R_{int} = 0.0899, R_{sigma} = 0.0846]
Data/restraints/parameters	4906/89/215
Goodness-of-fit on F^2	1.027
Final R indexes [I>=2σ (I)]	R_1 = 0.0622, wR_2 = 0.1449
Final R indexes [all data]	R_1 = 0.1030, wR_2 = 0.1647
Largest diff. peak/hole / e Å^{-3}	2.57/-1.47
Flack parameter	-0.06(7)

Details of crystal structure refinement: All non-hydrogen atoms were refined anisotropically. Hydrogen atoms were assigned to idealized geometric positions and included in structure factors calculations. SIMU, RIGU SADI and FLAT commands as implemented in the FragmentDB / DSR[3] were used on the atoms of the pyridinium cation which is disordered about the center of inversion.

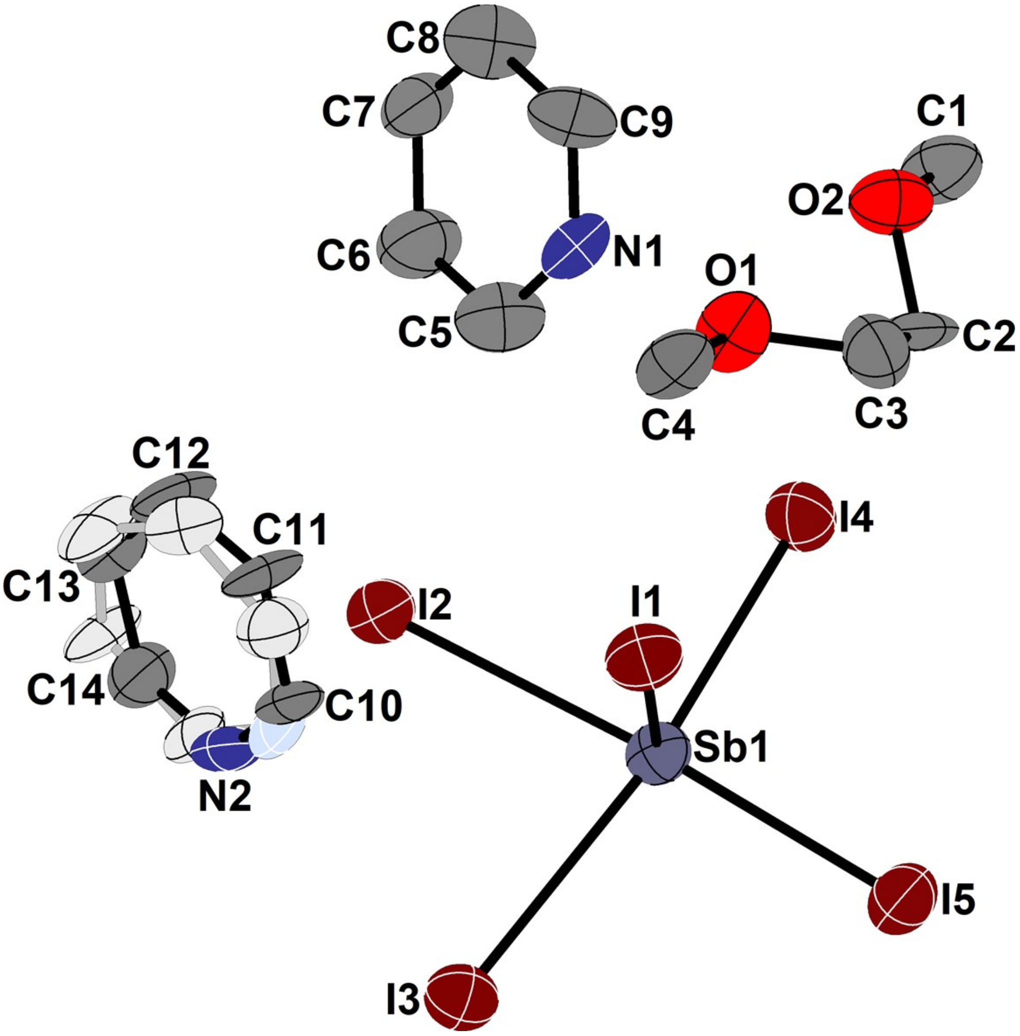

Figure S6: Asymmetric unit of **3-Sb**, ellipsoids at 50 % probability. Hydrogen atoms are omitted for clarity. The second position of the disordered pyridinium moiety is shown in lighter colors.

Table S7: Crystallographic data for $C_9H_{16}Bi_2I_7NO_2$ (**4**), measured on a Stoe IPDS-2/2T at 100 K, CCDC 2025575.

Empirical formula	$C_9H_{16}Bi_2I_7NO_2$
Formula weight	1476.49
Crystal system	triclinic
Space group	*P*-1
a/Å	10.7505(7)
b/Å	11.6799(8)
c/Å	13.0200(13)
α/°	102.317(7)
β/°	111.546(7)
γ/°	109.350(5)
Volume/Å^3	1326.1(2)
Z	2
ρ_{calc}/g/cm^3	3.698
μ/mm^{-1}	21.403
F(000)	1260.0
Crystal size/mm^3	0.147 × 0.142 × 0.051
Absorption correction (T_{min}/T_{max})	numerical (0.0560/0.3634)
2Θ range for data collection/°	3.638 to 53.79
Index ranges	$-13 \leq h \leq 13$, $-14 \leq k \leq 14$, $-16 \leq l \leq 16$
Reflections collected	34488
Independent reflections	5671 [R_{int} = 0.0827, R_{sigma} = 0.0509]
Data/restraints/parameters	5671/0/192
Goodness-of-fit on F^2	0.935
Final R indexes [I>=2σ (I)]	R_1 = 0.0246, wR_2 = 0.0459
Final R indexes [all data]	R_1 = 0.0425, wR_2 = 0.0482
Largest diff. peak/hole / e Å^{-3}	1.31/-0.92

Details of crystal structure refinement: All non-hydrogen atoms were refined anisotropically. Hydrogen atoms were assigned to idealized geometric positions and included in structure factors calculations.

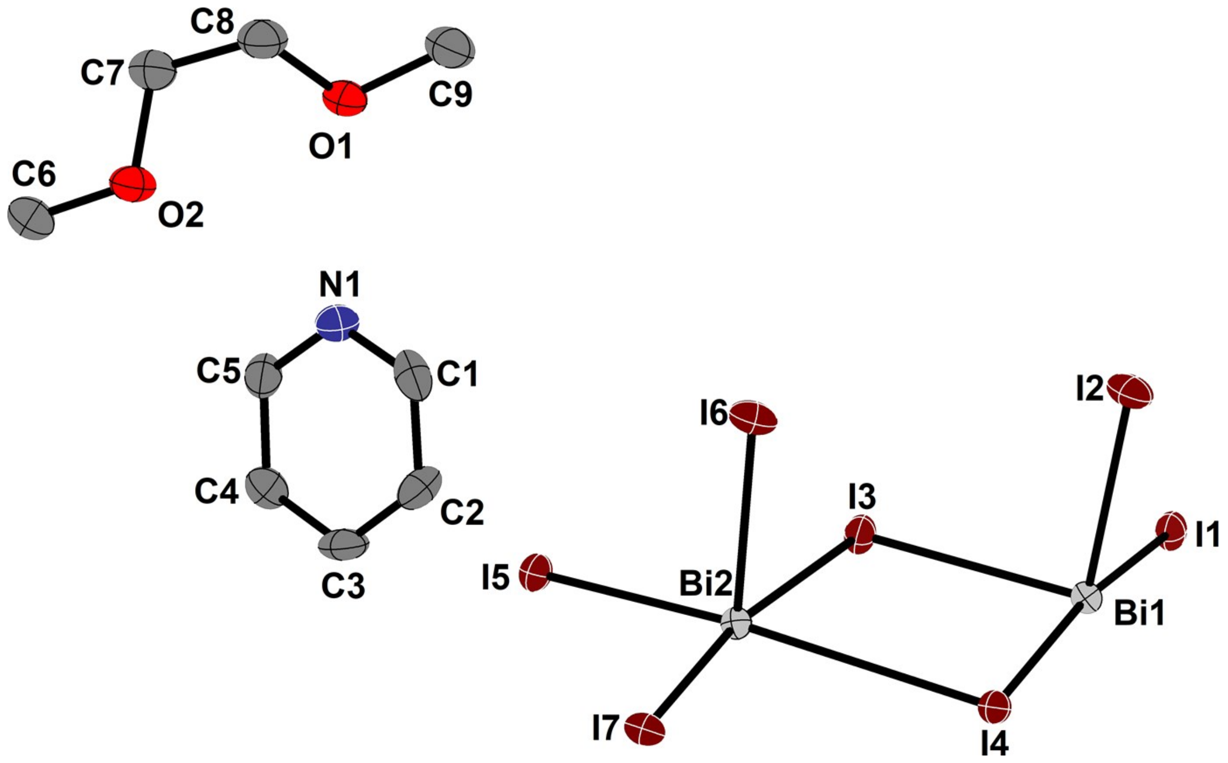

Figure S7: Asymmetric unit of **4**, ellipsoids at 50 % probability. Hydrogen atoms are omitted for clarity.

Table S8: Crystallographic data for $C_{36}H_{64}Bi_6I_{22}N_4O_8$ (**5**), measured on a Stoe IPDS-2/2T at 100 K, CCDC 2025576.

Empirical formula	$C_{36}H_{64}Bi_6I_{22}N_4O_8$
Formula weight	4726.59
Crystal system	monoclinic
Space group	$P2_1/c$
a/Å	19.4579(8)
b/Å	19.9643(6)
c/Å	12.4327(5)
α/°	90
β/°	107.255(3)
γ/°	90
Volume/Å^3	4612.3(3)
Z	2
ρ_{calc}g/cm^3	3.403
μ/mm^{-1}	18.804
F(000)	4072.0
Crystal size/mm^3	0.202 × 0.193 × 0.169
Absorption correction (T_{min}/T_{max})	multi-scan (0.0000/0.0012)
2Θ range for data collection/°	2.484 to 53.874
Index ranges	$-24 \leq h \leq 24$, $-25 \leq k \leq 23$, $-15 \leq l \leq 15$
Reflections collected	94343
Independent reflections	9860 [$R_{int} = 0.0706$, $R_{sigma} = 0.0351$]
Data/restraints/parameters	9860/0/347
Goodness-of-fit on F^2	1.009
Final R indexes [I>=2σ (I)]	$R_1 = 0.0328$, $wR_2 = 0.0792$
Final R indexes [all data]	$R_1 = 0.0471$, $wR_2 = 0.0819$
Largest diff. peak/hole / e Å^{-3}	2.12/-1.03

Details of crystal structure refinement: All non-hydrogen atoms were refined anisotropically. Hydrogen atoms were assigned to idealized geometric positions and included in structure factors calculations.

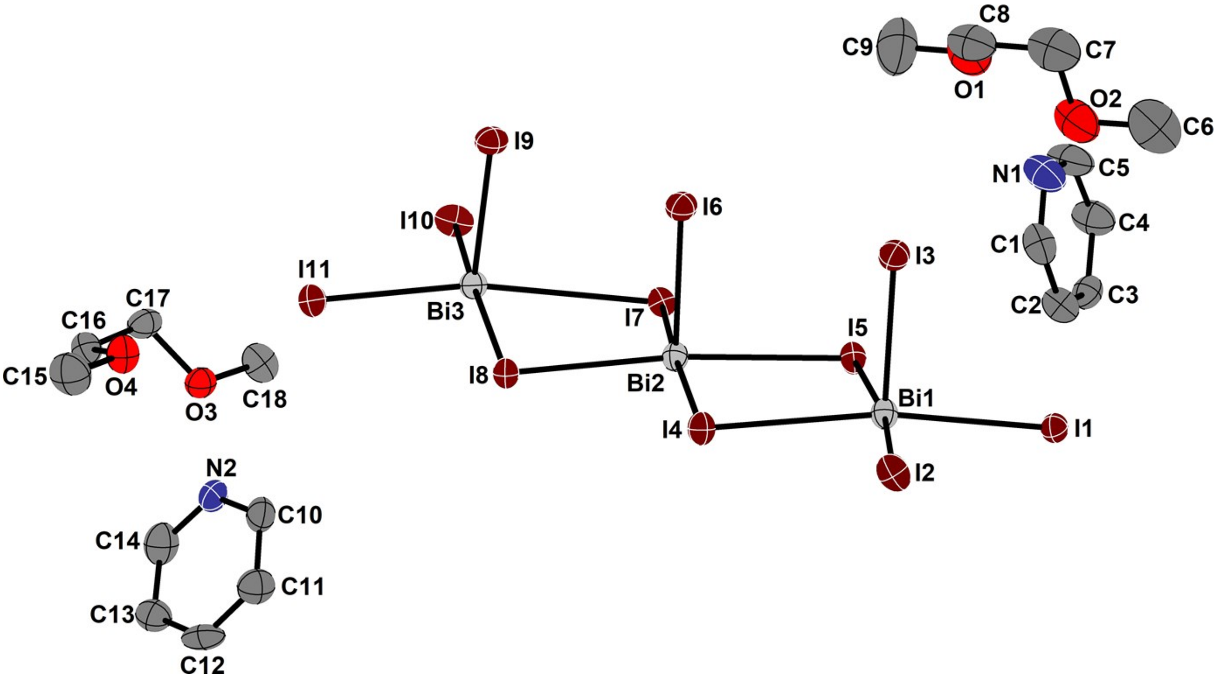

Figure S8: Asymmetric unit of **5**, ellipsoids at 50 % probability. Hydrogen atoms are omitted for clarity.

Table S9: Crystallographic data for $C_{20}H_{24}Bi_2I_{14}N_4$ (**6**), measured on a Stoe IPDS-2/2T at 100 K, CCDC 2025569.

Empirical formula	$C_{20}H_{24}Bi_2I_{14}N_4$
Formula weight	2514.99
Crystal system	orthorhombic
Space group	*Pnma*
a/Å	18.3316(10)
b/Å	32.7986(14)
c/Å	8.1963(3)
α/°	90
β/°	90
γ/°	90
Volume/Å^3	4928.0(4)
Z	7
ρ_{calc}g/cm^3	3.390
μ/mm^{-1}	15.921
F(000)	4320.0
Crystal size/mm^3	0.157 × 0.102 × 0.092
Absorption correction (T_{min}/T_{max})	multi-scan (0.0004/0.2186)
2Θ range for data collection/°	2.484 to 53.874
Index ranges	$-23 \leq h \leq 23$, $-37 \leq k \leq 41$, $-10 \leq l \leq 10$
Reflections collected	83000
Independent reflections	5406 [$R_{int} = 0.0960$, $R_{sigma} = 0.0352$]
Data/restraints/parameters	5406/0/190
Goodness-of-fit on F^2	1.072
Final R indexes [I>=2σ (I)]	$R_1 = 0.0714$, $wR_2 = 0.2239$
Final R indexes [all data]	$R_1 = 0.1027$, $wR_2 = 0.2374$
Largest diff. peak/hole / e Å^{-3}	5.26/-2.04

Details of crystal structure refinement: All non-hydrogen atoms were refined anisotropically. Hydrogen atoms were assigned to idealized geometric positions and included in structure factors calculations. Since two of the pyridinium cations are disordered about the center of an inversion, C1 and N1 as well as C4 and N3 share the same positions and all have an occupancy of 0.5. EXYZ and EADP commands were used to refine these positions. I8 has an occupancy of 0.5 as it is part of a disordered I_5^--anion.

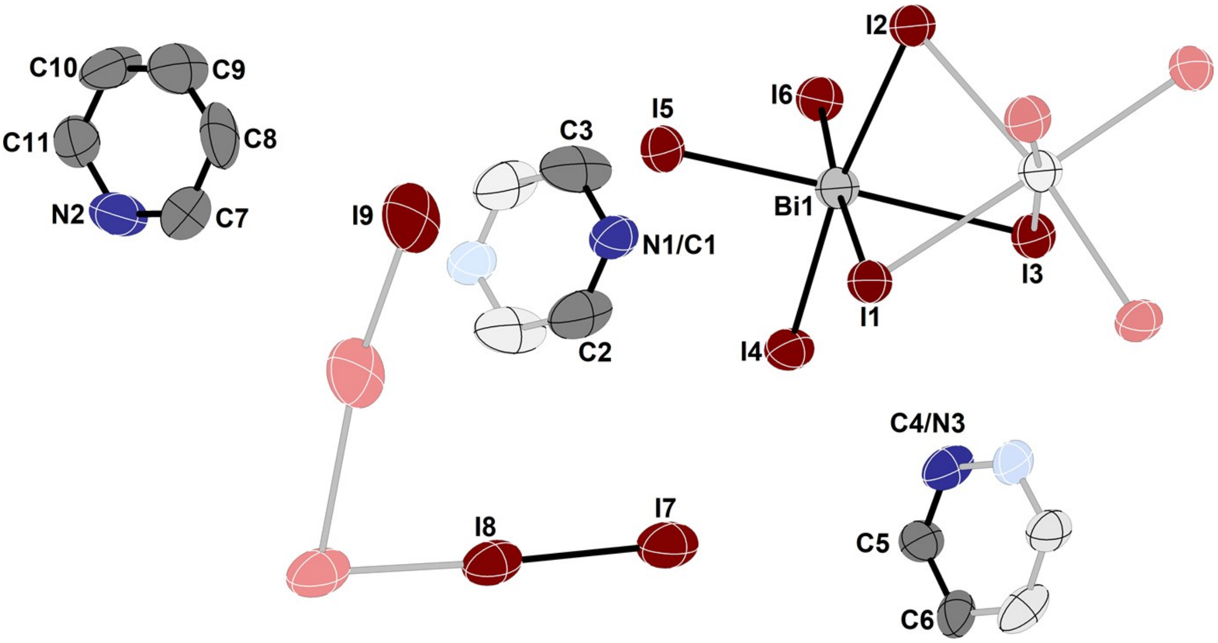

Figure S9: Excerpt of the crystal structure of **6**, ellipsoids at 50 % probability. Atoms that do not belong to the asymmetric unit are shown in lighter colors. Hydrogen atoms are omitted for clarity.

Powder Diffraction

Powder patterns were recorded on a *STADI MP* (*STOE* Darmstadt) powder diffractometer, with CuK$_{\alpha1}$ radiation with λ = 1.54056 Å at room temperature in transmission mode. The patterns confirm the presence of the respective phase determined by SCXRD measurements and the absence of any major crystalline by-products unless otherwise indicated.

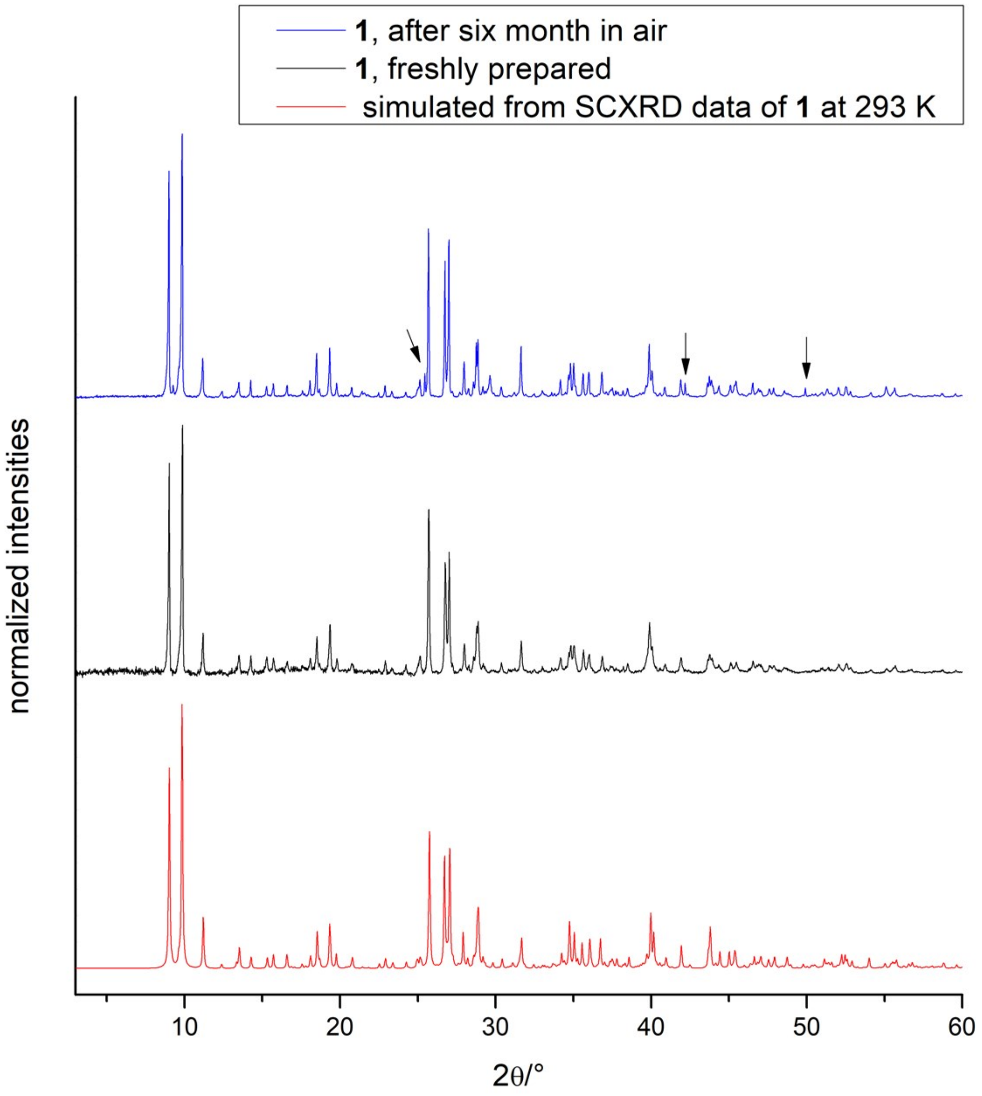

Figure S10. Powder diffraction patterns of $(HPy)_2(Py)CuBi_3I_{12}$ (**1**). The highlighted reflexes in the first pattern are due to impurities of CuI that come from the still un-optimized synthesis conditions in the first runs of preparation, rather than decomposition. The sample of the second pattern was prepared later on, using optimized conditions.

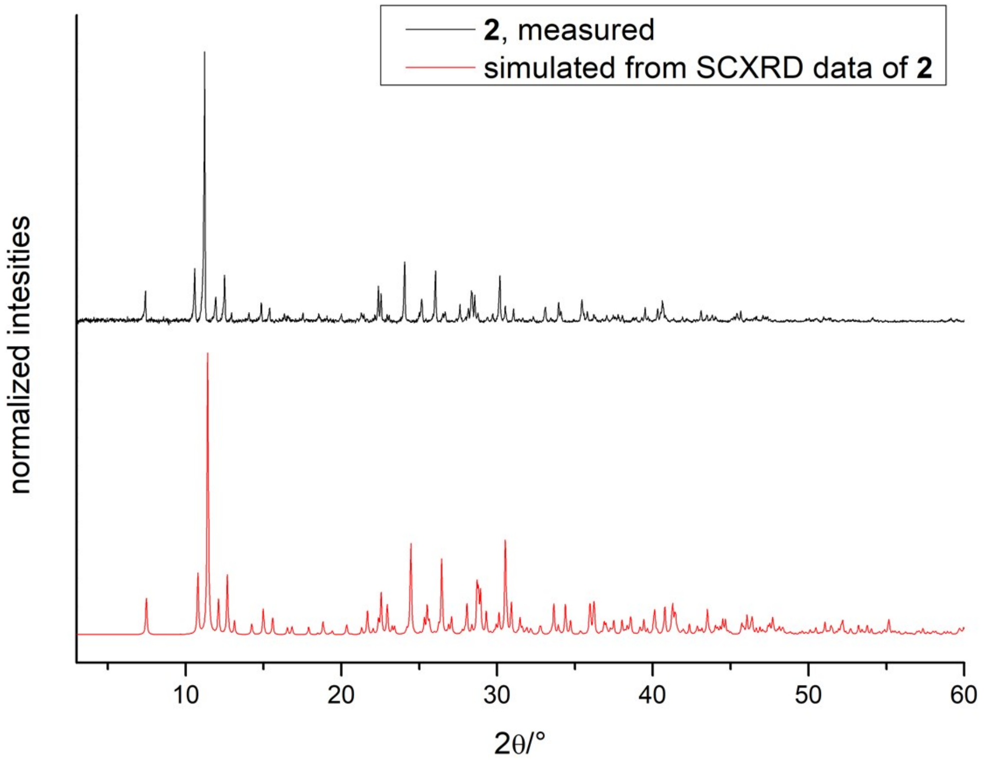

Figure S11. Powder diffraction pattern of $(HPy)_3Bi_2I_9$ (**2**).

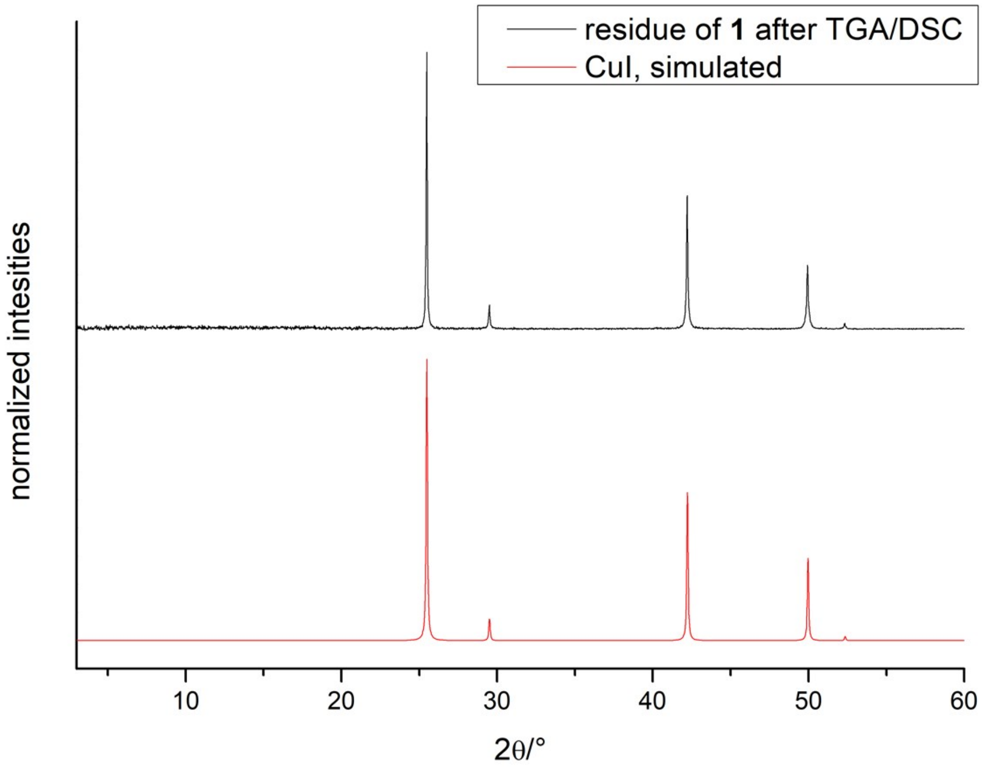

Figure S12. Powder diffraction pattern of the residue of **1** after heating to 550 °C under constant flow of N_2-gas during TGA/DSC measurments. The reference pattern is simulated from literature data.[4]

Thermal Analysis

The thermal behavior of $(HPy)_2(Py)CuBi_3I_{12}$ (**1**), was studied by TGA/DSC both on the crystals grown from dme/*n*-pentane solution as well as the bulk material precipitated from ethanol. The experiments were carried out on a NETSCH STA 409 C/CD with a heating rate of 10 °C/min in a constant flow of 80 ml/min N_2.

For the crystalline sample a temperature range from 20 °C to 1000 °C was used. A two-step mass loss of 91.4 % is observed between 150 °C and 500 °C. This corresponds to the complete decomposition of the product leaving only CuI behind. This residue completely decomposes in a second mass loss between 550 °C and 800 °C (see figure S13a).
For the analysis of the bulk material we chose a temperature range from 20 °C to 550 °C to be able to confirm *via* PXRD that the residue at 550 °C is CuI (see figure S12). In this case the main mass loss was observed to be 93.6 % (see figure S13b).

Since the residue at 550 °C is CuI, it is possible to directly determine the average occupation of the copper position in the crystal structure. For the crystalline product a share of 8.6 % of copper iodide of the whole substance corresponds to an occupation of 55 % on the copper position for which the theoretical share is 8.52 %. This is well in line with the values of 50 % and 60 % found in the two single crystal measurements.

However, the residue in the thermal analysis of the bulk product is only 6.4 % of the initial sample. A share of 6.4 % CuI of the whole substance points to an occupation of 40 % on the copper positions for which the theoretical share is 6.2 %.

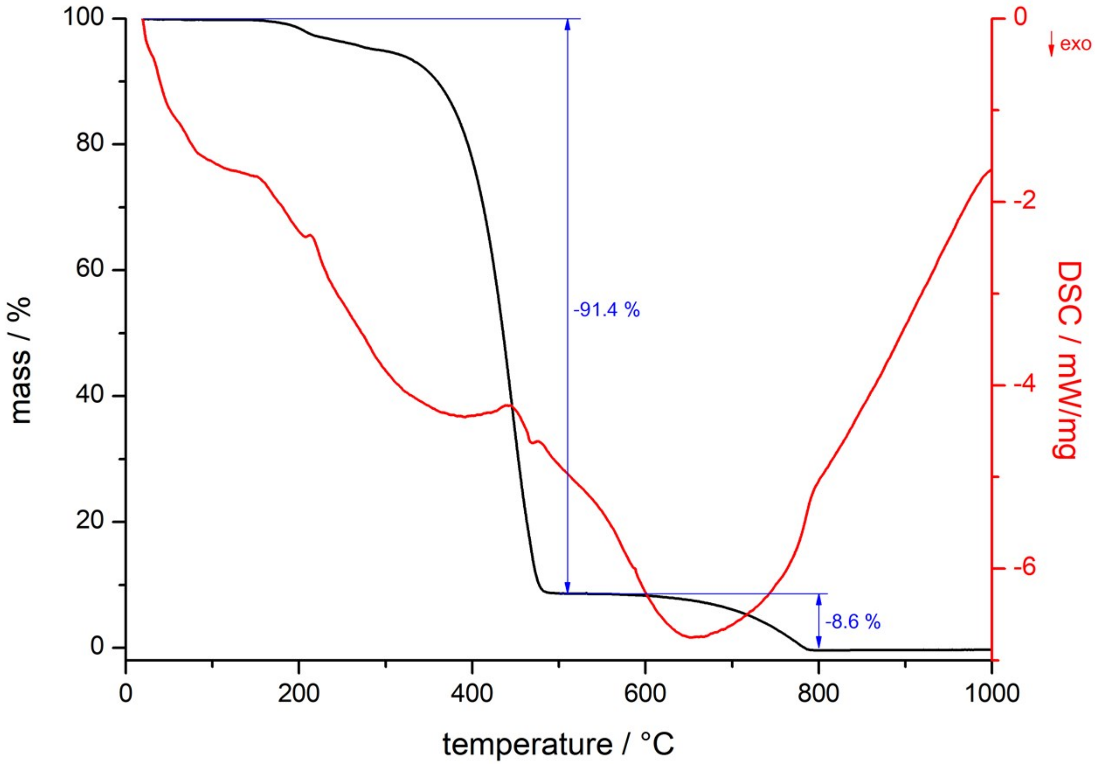

Figure S13a. TGA/DSC of $(HPy)_2(Py)CuBi_3I_{12}$ (**1**) (16.5 mg), grown as single crystals from dme/*n*-pentane.

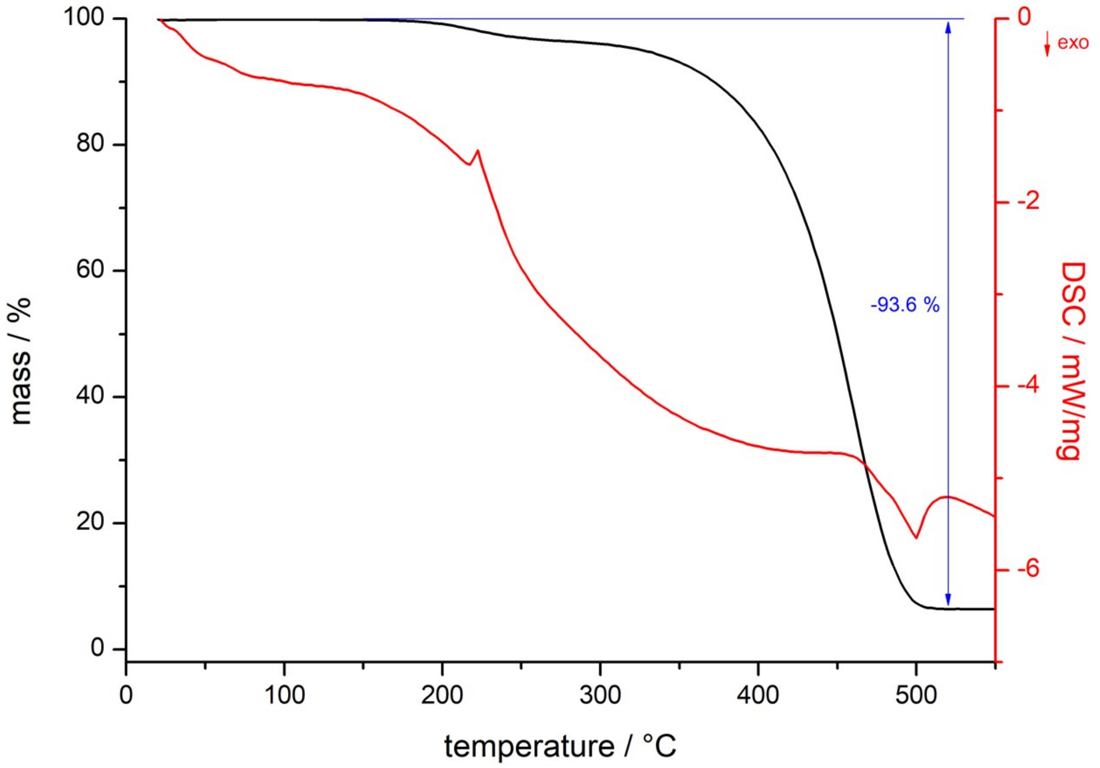

Figure S13b. TGA/DSC of $(HPy)_2(Py)CuBi_3I_{12}$ (**1**) (17.4 mg), produced as a bulk material from ethanol.

Optical properties

Optical absorption spectra were recorded on a Varian Cary 5000 UV/Vis/NIR spectrometer in diffuse reflectance mode employing a Praying Mantis accessory (Harrick). For ease of viewing, raw data was transformed from % Reflectance R to Absorbance A according to A = log (1/R).[5]

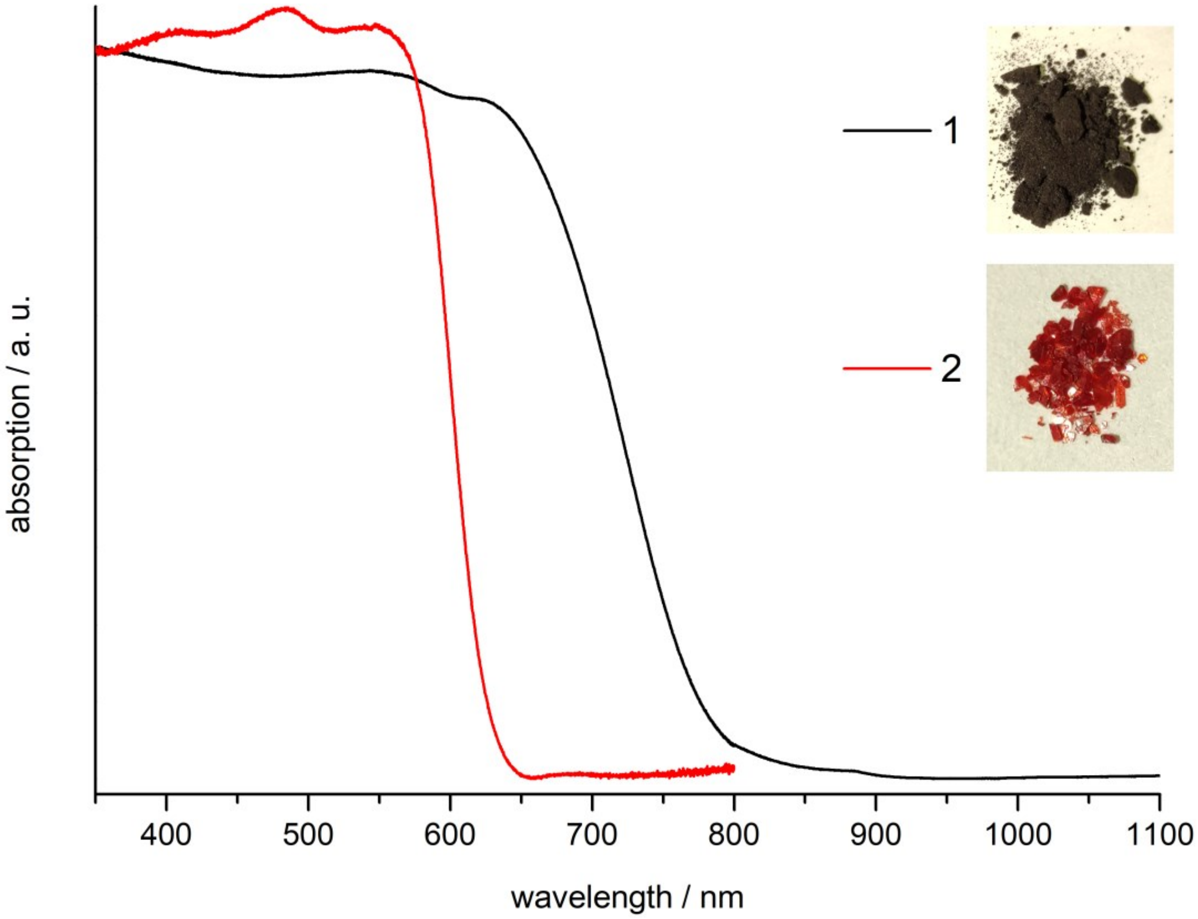

Figure S14. Optical absorption spectra of $(HPy)_2(Py)CuBi_3I_{12}$ (**1**) and $(HPy)_3Bi_2I_9$ (**2**) prepared as pure phases, measured in diffuse reflectance in the range of 350 nm to 1100 nm and 350 nm to 800 nm, respectively. Photographs of the products are shown as insets.

IR spectroscopy

IR spectra were recorded on a *Bruker Tensor 37* FT-IR spectrometer equipped with an ATR-Platinum measuring unit.

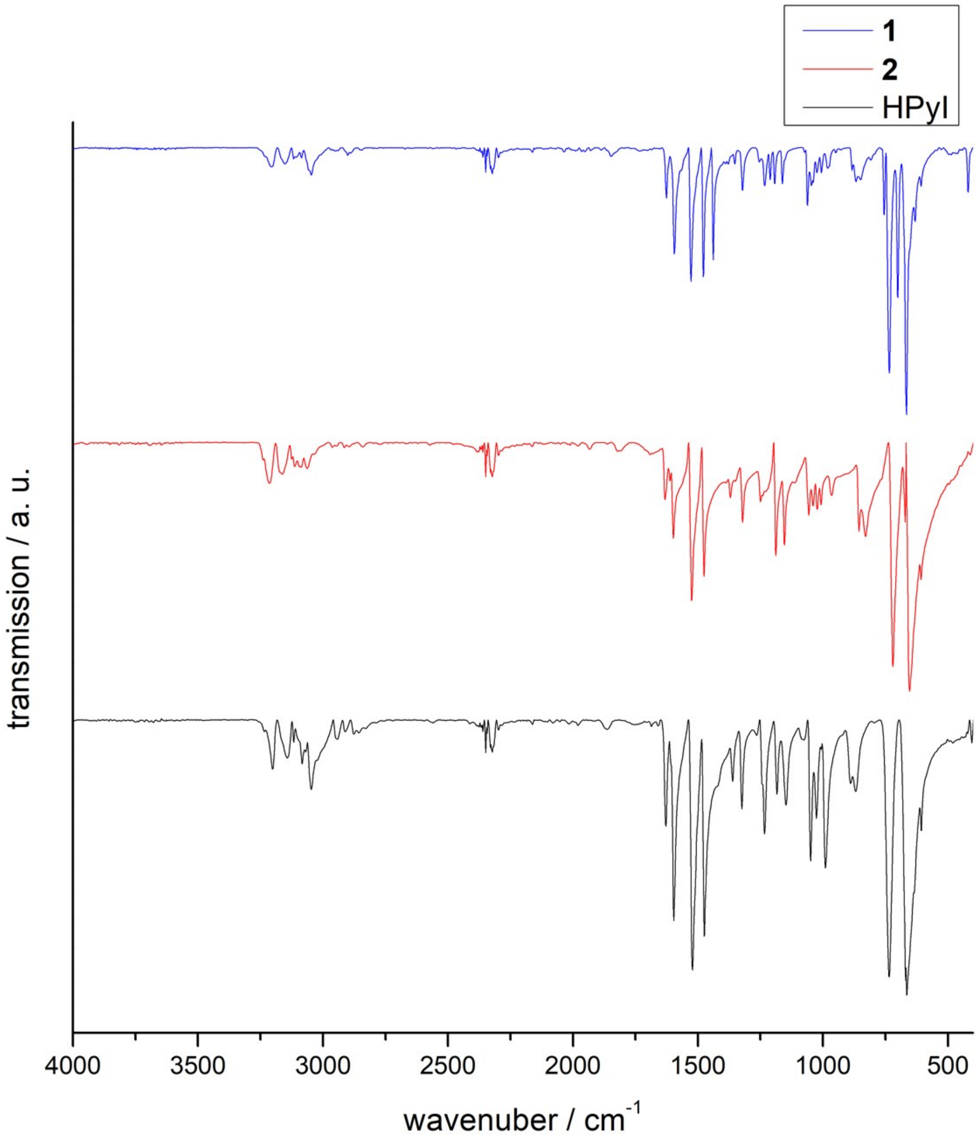

Figure S15. IR spectrum of **1**, **2** and HPyI, measured form 4000 – 400 cm^{-1}. The predominant bands at 3300 – 3000 cm^{-1} can be assigned to the N-H and C-H vibrations of the pyridinium and in case of **1** also pyridine moieties. The strongest of those bands at 3047 cm^{-1} in the spectra of **1** and HPyI can be assigned to the C-H-valence vibration. The group of bands around 2300 cm^{-1} are an artefact of the atmospheric CO_2 compensation applied by the spectrometer software.

Photoconductivity Measurements

For measurements of the photoconductivity, pellets of about 1.3 cm in diameter were produced from compound **1** and contacted with two measuring tips. To improve the electrical contact, conductive silver paint was used. The distance between the two contact points was about 1 mm. For photocurrent measurements, a bias of 10 V was applied and the material was excited with a helium neon laser with an operation wavelength of 632.8 nm. With a variable grey attenuation filter, different excitation powers were set ranging from 8 to 200 µW. To measure the small current signals in the range of picoamperes, the laser beam was modulated with an optical chopper at 670 Hz and the photocurrent was amplified with a current amplifier (Femto), before it was detected with a lock-in amplifier (Stanford SR 830). The integration time for each measurement was 1 s and the datapoints presented in Figure 4 were averaged over a number of 13 measurements.

References

[1] Brauer, G., Ed. Handbuch der Präparativen Anorganischen Chemie, 3rd ed., Ferdinand Enke Verlag: Stuttgart, Germany, **1975**, Vol. 1, 600.

[2] Chai, W.-X.; Wu, L.-M.; Li, J.-Q.; Chen, L. A Series of New Copper Iodobismuthates: Structural Relationships, Optical Band Gaps Affected by Dimensionality, and Distinct Thermal Stabilities. *Inorg. Chem.* **2007**, *46*, 8698-8704.

[3] Kratzert, D.; Holstein, J. J.; Krossing, I. *J. Appl. Crystallogr.* **2015**, *48*, 933-938.

[4] Wyckoff, R. W. G.; Posnjak, E. The crystal structures of the cuprous halides. *J. Am. Chem. Soc.* **1922**, *44*, 30-36.

[5] Boldish, S. I.; White, W. B. Optical band gaps of selected ternary sulfide minerals. *Am. Mineral.* **1998**, *83*, 865-871.